Backstepping-Based Quasi-Sliding Mode Control and Observation for Electric Vehicle Systems: A Solution to Unmatched Load and Road Perturbations

World Electric Vehicle Journal

MDPI

Article

Backstepping-Based Quasi-Sliding Mode Control and Observation for Electric Vehicle Systems: A Solution to Unmatched Load and Road Perturbations

Akram Hashim Hameed [1,2], Shibly Ahmed Al-Samarraie [2], Amjad Jaleel Humaidi [2,*] and Nagham Saeed [3]

[1] Al-Sader Branch, Baghdad State Company of Electricity Distribution, Ministry of Electricity, Baghdad 10066, Iraq; cse.21.03@grad.uotechnology.edu.iq
[2] Control and System Engineering Department, University of Technology, Baghdad 10066, Iraq; shibly.a.alsamarraie@uotechnology.edu.iq
[3] School of Computing and Engineering, University of West London, London W5 5RF, UK; nagham.saeed@uwl.ac.uk
* Correspondence: amjad.j.humaidi@uotechnology.edu.iq

Abstract: The direct current (DC) motor is the core part of an electrical vehicle (EV). The unmatched perturbation of load torque is a challenging problem in the control of an EV system driven by a DC motor and hence a deep control concern is required. In this study, the proposed solution is to present two control approaches based on a backstepping control algorithm for speed trajectory tracking of EVs. The first control design is to develop the backstepping controller based on a quasi-sliding mode disturbance observer (BS-QSMDO), and the other controller is to combine the backstepping control with quasi-integral sliding mode control (BS-QISMC). In the sense of Lyapunov-based stability analysis, the ultimate boundedness of the proposed controllers has been detailedly analyzed, assessed, and evaluated in the presence of unmatched perturbation. A modified stability analysis has been presented to determine the ultimate bounds of disturbance estimation error for both controllers. The determination of ultimate bound and region-of-attraction for tracking and estimation errors is the contribution achieved by the proposed control design. The performances of the proposed controllers have been verified via computer simulations and the level of ultimate bounds for the estimation and tracking errors are the key measures for their evaluation. Compared to BS-QISMC, the results showed that a lower level of ultimate boundedness with a higher convergent rate can be reached based on BS-QSMO. However, a higher control effort can be exerted by the BS-QSMO controller as compared to BS-QISMC; and this is the price to be paid by the BS-QSMO controller to achieve lower ultimate boundedness with a faster convergence rate.

Keywords: electrical vehicle system; quasi-sliding mode disturbance observer; global stabilization; unmatched disturbance perturbation; quasi-integral sliding mode control

Citation: Hameed, A.H.; Al-Samarraie, S.A.; Humaidi, A.J.; Saeed, N. Backstepping-Based Quasi-Sliding Mode Control and Observation for Electric Vehicle Systems: A Solution to Unmatched Load and Road Perturbations. *World Electr. Veh. J.* **2024**, *15*, 419. https://doi.org/10.3390/wevj15090419

Academic Editor: Yujie Wang

Received: 30 July 2024
Revised: 1 September 2024
Accepted: 9 September 2024
Published: 14 September 2024

1. Introduction

In order to ensure a clean climate and to account for the reduction of fossil fuels, internal combustion engines are being gradually replaced by electric drive systems in most life facilities. The technology of electric vehicles (EVs) is a suitable and efficient solution due to its reliability and sustainability. In 2020, the global electric car stock hit the 10 million mark, a 43% increase over 2019, and representing a 1% stock share. Battery electric vehicles (BEVs) accounted for two-thirds of new electric car registrations and two-thirds of the stock in 2020 [1–3]. Figure 1 illustrates the market share of EVs in comparison to the other fuel vehicles [3].

In general, to actuate electric vehicles, different types of electric motors can be used like DC motors, synchronous motors, induction motors, and reluctance motors [4]. Moreover, it is important to note that, by virtue of vector control theory, the control of any type of

electric actuator, like induction, synchronous, and reluctance motors, is converted to DC-like motors. Due to its simplicity, ease of manufacturing, and maintenance, the DC motor is a suitable choice for most EV applications [5]. The weight of passengers and the disturbances due to bumpy roads are the potential uncertainties encountering the speed control of EVs. In spite that, the DC motor model is easy to develop, the presence of unmatched perturbation represents a challenging problem when evaluating the performance of robust controllers in terms of load torque [1]. To tackle the perturbation problem, one may use disturbance estimation together with the proposed controller to compensate for the mismatched perturbation as a hard solution. The other solution is to design a control law that can only reduce the effect of perturbation. However, the assessment of the proposed control solution depends on how it can reduce the ultimate bound of convergence error [2]. The recent combination of a backstepping controller with an observer or robust controller could effectively tackle this problem and provide improved robust characteristics.

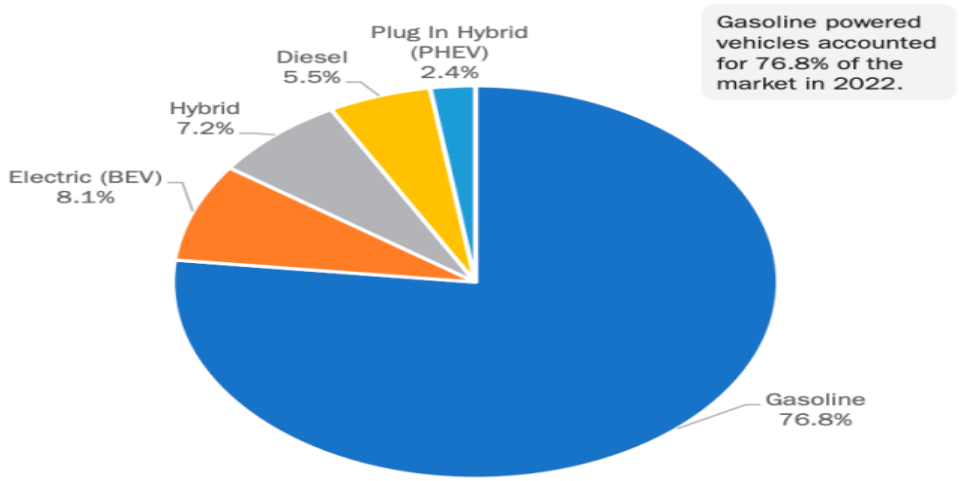

Figure 1. EV market share versus other fuel vehicles.

Backstepping control (BS) is an efficient technique that belongs to a class of nonlinear control approaches that could stabilize complex systems with nonlinear dynamics [6]. The main concept of the BS control algorithm is based on subdividing the overall system into sub-channels and converting the control objective into a series of individual, interconnected control tasks by stepping back through these channels [7,8]. Virtual control laws are introduced within the interconnected subsystems such that the stability of nonlinear strict-feedback systems is guaranteed and the design is straightforward [9,10]. Unfortunately, the robustness characteristics of BS-controlled nonlinear systems subjected to unmatched perturbations are not guaranteed and studies are continuing to boost this property.

Generally, the perturbations of nonlinear systems can be classified as vanishing and non-vanishing perturbations according to their effectiveness in the equilibrium set [11]. In the sense of their impacts on the controller column space, they are also divided into matched and unmatched perturbations [12,13]. Non-vanishing unmatched perturbations are the worst perturbation structures for which a deep control concern is required to compensate. Previous studies have shown that the best control design could lead to uniform ultimate boundedness of states (errors). In this sense, the competition of controllers is based on how well one can give the least ultimate bound [9,14,15].

The use of a BS control algorithm cannot solve the problem of a controlled system with unmatched perturbations unless it is fused with another robust controller or disturbance observer to improve its robustness characteristics [16,17]. In this sense, previous control frameworks have recently been proposed to tackle this problem such as higher-order adaptive SMC perturbation estimation [15], a hierarchal quasi-continuous HOSM controller [18], backstepping based on sigmoid SMC [19], nonlinear disturbance observer-based backstepping [16,20,21], and ISMC mixed H_∞ control [22].

The merging of disturbance observers to the BS algorithm is one of the effective solutions to the problem of unmatched uncertainties [23,24]. Among many observers in the literature, the sliding mode disturbance observer (SMO) is one of the most efficient observers. It is synthesized based on the equivalent control principle and it results in an exact estimation of system perturbation. The SMO can be designed in two phases: the reaching phase and the sliding phase. In the reaching phase, the estimation error trajectory moves towards the sliding manifold, and when the sliding variable (trajectory) reaches the sliding manifold the sliding phase begins [25,26]. In the sliding phase, the trajectory will remain on the sliding manifold and be guided to the equilibrium point which represents zero estimation error [27,28]. The price to be paid to have high performance in terms of estimation error is the appearance of chattering behavior due to the discontinuous injection term of the observer [29,30]. The use of filters to eliminate the chattering high-frequency components may lead to increased complexity of system dynamic [12,31,32]. As such, due to this inherited chattering phenomenon, the SMO cannot be used as a virtual controller in the backstepping algorithm since it will generate high-frequency chattered virtual-control laws through the steps of backstepping control design. Therefore, one needs to propose another version of SMO that can eliminate both the reaching phase and chattering phenomenon without using filtering design [33–35]. This objective can be satisfied by introducing the quasi-tanh-based SMO [36,37]. Accordingly, this study has proposed a backstepping controller based on quasi-SMO to solve the problem of unmatched perturbation.

The fusing of the BS algorithm to other robust controllers is an alternative solution to solving the problem of unmatched perturbation [38,39]. In this study, integral sliding mode control (ISMC) has been proposed as an efficient candidate to be combined with the BS algorithm. ISMC is an improved version of conventional SMC, which works to eliminate the reaching phase. In an ISMC controller, the sliding phase begins from the first moment of trajectory startup [40,41]. Consequently, the perturbation is rejected from the first instant. However, auxiliary dynamics have to be added to the system dynamics to achieve this improved performance of ISMC. Nevertheless, the control action still contains high-frequency components and the chattering cannot be avoided [42,43]. Again, the quasi (tanh) ISMC is proposed to eliminate the chattering phenomenon.

In this work, the problem of speed trajectory tracking control for EV DC drive systems subjected to unmatched load torque will be addressed and assessed based on disturbance-based backstepping control methodologies. Two backstepping control schemes are proposed, represented by a quasi-sliding mode disturbance observer-based backstepping controller (BS-QSMO), and backstepping based quasi-integral sliding mode control (BS-QISMC). The design and stability analysis are developed to ensure the ultimate boundedness of tracking and estimation convergence errors. In addition to the conventional backstepping control algorithm, the proposed controllers are compared in terms of tracking and estimation convergence errors. The main challenging task of these controllers is how to manage the unmatched disturbance in the framework of backstepping control. Figure 2 presents the schematic configuration of the proposed backstepping controller based on the two disturbance observers for an EV based on a DC drive control system. In this configuration, a one-motor drive with a differential is assumed. Nevertheless, a four-motor drive (one motor for each wheel) is a case that leads to what is called a quarterly traction EV. However, this study will be concerned with speed control of the driving motor of one motor drive with a differential configuration EV.

The following literature highlights briefly the previous studies that were undertaken to control different DC-actuated systems. In [44], an integral nonlinear controller is designed for DC motors affected by an external load, the integral term is considered as a saturation error function to gain robust properties against the external torque. In [45], backstepping based on the nonlinear PI controller is used for the DC motor. In [46], DC motor speed control with load torque is considered and a robust MRAC is designed and tested. In [47], an optimized PID controller is considered for the DC motor with a heuristic optimization

algorithm named Harris Hawk's Optimization (HHO) algorithm. In [48], the speed control of a brushed DC motor is implemented with the manually tuned PID control algorithm. In [49], fixed point induction and zero average dynamics and controllers driving a buck converter for DC motor speed control are designed. In [50], fuzzy controller-based genetic algorithm optimization is considered for DC motors. In [51], robust tracking performance and regulatory effective control for a brushed DC motor are designed and assessed based on active disturbance reduction of the linear extended observer. In [52], the trajectory tracking of rotor angular velocity for a converter-fed system DC motor with load torque is designed using a continuous nonsingular terminal sliding mode control. In [53], adaptive law-based backstepping cooperated with integral sliding mode control of the angular speed control of a DC motor with an external load is designed. In [54], a comparative control analysis of P, PI, and PID is conducted. In [55], velocity trajectory tracking of a DC motor based on hierarchical flatness control is addressed. In [56], fractional order PID tuning and design for an electric vehicle drive based on a DC motor is designed and tuned.

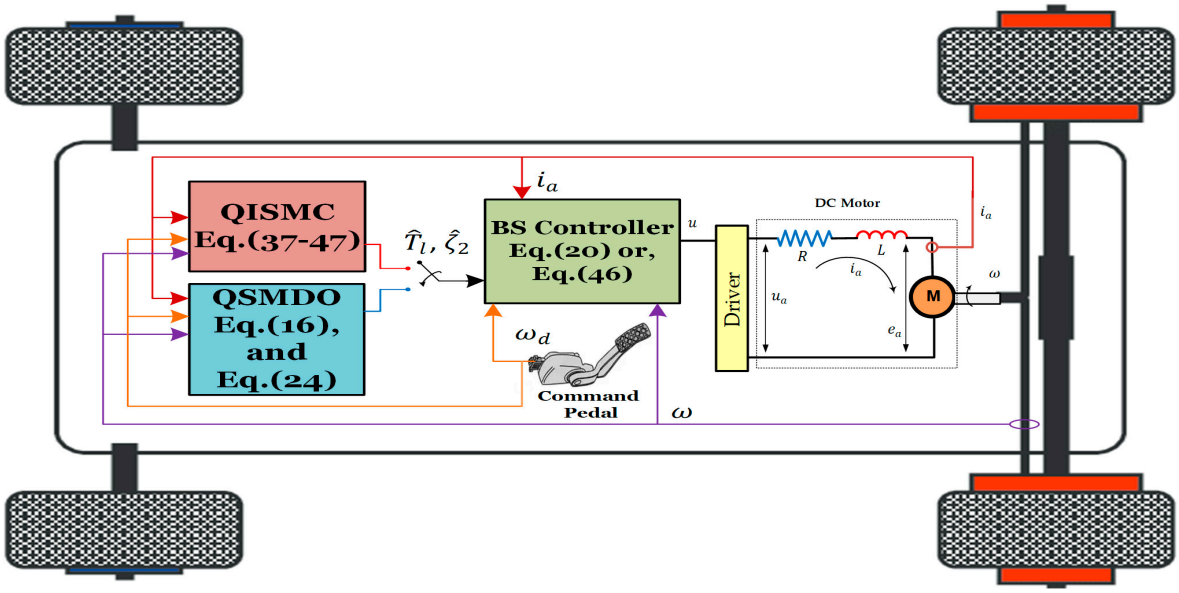

Figure 2. The proposed control schemes.

The main objective of this paper is to design two backstepping control schemes; one is based on a quasi-sliding mode observer and the other is based on a quasi-integral sliding mode controller for speed trajectory tracking control of a DC motor-actuated EV system subjected to unmatched load torque. The contribution of this study can be stated in the following points:

- Development of backstepping based on a quasi-sliding mode disturbance observer (BS-QSMO) using Lyapunov stability. The key contribution of this part is to conduct a rigorous mathematical analysis to determine the ultimate bound of disturbance estimation error;
- Development of a backstepping control algorithm based on the quasi-integral sliding mode control (BS-QISMC) using Lyapunov stability analysis. The key contribution of this part is to conduct a rigorous mathematical analysis to determine the ultimate bound of disturbance estimation error;
- Conducting a comparison study of the performance of the two proposed controllers.

2. Mathematical Modelling and Problem Formulation

The DC motor is the main part of an EV which works to convert the electric energy to mechanical torque and speed. In this paper, a separately-excited armature control DC

motor has been applied for vehicle actuation. According to Newton's second law and Kirchhoff's voltage law (KVL), the following model can be established [1]

$$\dot{x}_1 = -a_1 x_1 + a_2 x_2 + d \tag{1}$$

$$\dot{x}_2 = -a_3 x_1 + a_4 x_2 + \frac{1}{L_a} u \tag{2}$$

where, $x_1 = \omega$ and $x_2 = i_a$, and i_a is the armature current, ω represents the armature angular speed, and L_a denotes the winding inductance of armature [57]. The disturbance (load torque) is represented by $d = \frac{1}{J} T_{l1}$ such that $|d| = \frac{1}{J}|T_{l1}| \leq d_1$, where d_1 is the upper bound of load torque. The parameters a_i $(i = 1, \cdots, 4)$ can be defined by $a_1 = b/J$, $a_2 = K_b/J$, $a_3 = K_b/L_a$, and $a_4 = K_b/R_a$, where R_a represents the resistance of the armature windings. The signal u represents the control action to actuate the DC motor system [58].

It is clear from Equations (1) and (2) that the model includes unmatched perturbation (load torque), which is considered a challenging control problem to be addressed in this study. Therefore, the control objective is to design an observer-based backstepping controller based on the above model to make x_1 track a desired trajectory x_{1d} in the presence of unmatched disturbance d with a known upper bound and the capability to measure all states [59].

The system of Equations (1) and (2) is in strictly in feedback form and the state transformation of $z_1 = x_1 - x_{1d}$, is applied, then

$$\dot{z}_1 = -a_1 x_1 + a_2 x_2 + d - \dot{x}_{1d} \tag{3}$$

Remark 1. *Acceptable convergence ultimate bound is a significant control objective where $|z_1| \leq \rho(d_1)$, where ρ is a K-class function that can be made arbitrarily small via a suitable selection of controller parameters to obligate it to stay in some neighborhood of zero, and d_1 is the upper bound of the perturbations or their first derivative.*

3. Controller Design

There are many control extensions of the backstepping algorithm that deal with unmatched disturbance. Fusing the observer techniques with the backstepping control could effectively tackle the unmatched problem, which motivated a rapid rise of observer-based backstepping control theory. In what follows, the backstepping control design based on three versions of observers will analyzed in detail for the DC drive system under unmatched disturbance (load torque).

3.1. Backstepping

For the system of Equations (1) and (2), a proposed virtual controller for the upper unperturbed sub-system of Equation (3) can take the form of:

$$x_2^* = -cz_1 - ax_1 + \dot{x}_{1d} \tag{4}$$

a Lyapunov candidate for the unperturbed sub-channel of Equation (3), with replacing x_2 by x_2^* of Equation (4) to have

$$V_{z_1} = \frac{1}{2} z_1^2 \tag{5}$$

$$\dot{V}_{z_1} = z_1\left(-a_1 x_1 - \dot{x}_{1d} + x_2^*\right)$$

or,

$$\dot{V}_{z_1} = z_1(-cz_1) = -cz_1^2 < 0 \qquad \forall z_1 \neq 0 \tag{6}$$

The second channel error is defined as $z_2 = x_2 - x_2^*$; hence,

$$\dot{z}_1 = -cz_1 + z_2 + d \tag{7}$$

The dynamics of z_2 can be expressed as

$$\dot{z}_2 = -a_3x_1 - a_4x_2 + \frac{1}{L_a}u - c^2z_1 + cz_2 + cd - a_1^2x_1 + a_1a_2x_2 + a_1d - \ddot{x}_{1d} \tag{8}$$

The overall Lyapunov candidate can be defined as,

$$V(z_1, z_2) = V_{z_1} + \frac{1}{2}z_2^2 = \frac{1}{2}\left(z_1^2 + z_2^2\right) \tag{9}$$

Taking the time derivative of $V(z_1, z_2)$ to get

$$\begin{gathered}\dot{V}(z_1, z_2) = -cz_1^2 + z_1d + z_2(-a_2a_3x_1 - a_2a_4x_2 + \frac{a_2}{L_a}u + (1 - c^2)z_1 + cz_2 + \\ cd - a_1^2x_1 + a_1a_2x_2 + a_1d - \ddot{x}_{1d})\end{gathered} \tag{10}$$

Let the lumped perturbations of the unmatched perturbation on the column space of the controller be represented by $\zeta_1 = (a_1 + c)d$, where $|\zeta_1| \leq \mu_1 > 0 \in R$, then a control law can be proposed as

$$u = \frac{L_a}{a_2}\left(-\left(1 - c^2\right)z_1 - 2cz_2 + \left(a_2a_3 + a_1^2\right)x_1 + a_2(a_4 - a_1)x_2 + \ddot{x}_{1d}\right) \tag{11}$$

Using Equation (11), Equation (10) becomes

$$\dot{V}(z_1, z_2) = -c\left(z_1^2 + z_2^2\right) + z_1d + z_2\zeta_1 \ \leq -c\,||z\,||^2 + \sqrt{|d|^2 + |\zeta_1|^2}\,||z\,|| \tag{12}$$

Let $||D_1\,|| = \sqrt{d_1^2 + \mu_1^2}$, and $0 < \vartheta < 1$, then according to [9],

$$\dot{V}(z_1, z_2) \leq -c(1 - \vartheta)\,||z\,||^2 + ||D_1\,||\,||z\,|| - c\vartheta\,||z\,||^2 \tag{13}$$

$$\dot{V}(z_1, z_2) \leq -c(1 - \vartheta)\,||z\,||^2 \quad \forall ||z\,|| > \frac{1}{c\vartheta}\,||D_1\,|| \tag{14}$$

Referring to [9] (Theorem 4.18 and Lemma 9.2), the tracking error uniform ultimate bound can be deduced to be

$$||z\,|| \leq \frac{1}{c\vartheta}\,||D_1\,|| \tag{15}$$

The uniform ultimate bound of Equation (15) reflects the challenge of this type of system addressed by this paper. In spite that, the BS controller could manage the upper system individually, a certain environment is a necessary condition to work properly. Hence, the best reachable uniform ultimate bound that the BS controller (mathematically) is depending on the upper bound of $||D_1\,||$, and the parameter c, which cannot be arbitrarily minimized.

3.2. Backstepping Controller Based on Quasi-Sliding Mode Disturbance Observer

In this part, two sub-observers are designed: one for the system channel of Equation (1) to account for unmatched disturbance. In contrast, the design of the other observer is devoted to coping with the projection of lumped disturbance to the second channel. Firstly, the observer of the first channel is designed based on Equation (1):

$$\dot{\hat{x}}_1 = -a_1x_1 + a_2x_2 + \hat{d} \tag{16}$$

The estimation error is defined by $\overline{x}_1 = x_1 - \hat{x}_1$ and its dynamics can be described by

$$\dot{\overline{x}}_1 = d - \hat{d} = \overline{d} \tag{17}$$

Selecting $\hat{d} = k_1 tanh(\overline{x}_1/\epsilon)$, where $1 \gg \epsilon > 0 \in R$, and $k_1 > 0 \in R$ are design parameters. The stability analysis based on the sliding mode theory leads to:

$$\overline{x}_1 \dot{\overline{x}}_1 \leq -|\overline{x}_1|(k_1 tanh(\overline{x}_1/\epsilon) - d) \tag{18}$$

where $k_1 > d_1$ is a necessary condition to satisfy Equation (18). Using the same procedure followed by Equations (11)–(15), to get

$$\dot{z}_1 = -cz_1 + z_2 + \overline{d} \tag{19}$$

$$u = \frac{L_a}{a_2}(u_1 + u_2) \tag{20}$$

where,

$$u_1 = \left(a_2 a_3 + a_1^2\right) x_1 - \left(1 - c^2\right) z_1 - 2cz_2 + a_2(a_4 - a_1)x_2 + \ddot{x}_{1d} + c\hat{d} \tag{21}$$

Hence,

$$\dot{z}_2 = -cz_2 - z_1 + u_2 + \dot{\hat{d}} + (c - a_1)\, d \tag{22}$$

letting $\zeta_2 = \dot{\hat{d}} + (c - a_1)d$, where $|\zeta_2| \leq \mu_2$, one can obtain

$$\dot{z}_2 = -cz_2 - z_1 + u_2 + \zeta_2 \tag{23}$$

The proposed structure of the second observer is designed as

$$\dot{\hat{z}}_2 = -cz_2 - z_1 + u_2 + \hat{\zeta}_2 \tag{24}$$

If $\hat{\zeta}_2$ is defined as $\hat{\zeta}_2 = k_2\, tanh(\overline{z}_2/\epsilon)$, where $k_2 > 0 \in R$ is a design parameter, then the dynamics of the estimation error is written as:

$$\dot{\overline{z}}_2 = \zeta_2 - \hat{\zeta}_2 = \overline{\zeta}_2 \tag{25}$$

One can establish the reaching condition as follows:

$$\overline{z}_2 \dot{\overline{z}}_2 \leq -|\overline{z}_2|(k_2 tanh(\overline{z}_2/\epsilon) - \zeta_2) \tag{26}$$

where $k_1 > d_1$ is required. If the control part is assigned as $u_2 = -\hat{\zeta}_2$, then

$$\dot{z}_2 = -cz_2 - z_1 + \overline{\zeta}_2 \tag{27}$$

Using the Lyapunov candidate as Equation (9), the $\dot{V}(z_1, z_2)$ becomes

$$\dot{V}(z_1, z_2) = -c\left(z_1^2 + z_2^2\right) + z_1\overline{d} + z_2\overline{\zeta}_2 \tag{28}$$

A uniform ultimate bound on $\overline{x}_1$ and $\overline{\zeta}_2$ can be deduced according to the following Lyapunov analysis

$$V_{\overline{x}_1} = \frac{1}{2}\dot{\overline{x}}_1^2 \tag{29}$$

$$\dot{V}_{\overline{x}_1} = \left(\dot{d} - \dot{\hat{d}}\right)\dot{\overline{x}}_1 \leq -\left|\dot{\overline{x}}_1\right|\left(\left|\dot{\hat{d}}\right| - \left|\dot{d}\right|\right) \tag{30}$$

Since $\hat{d} = k_1 tanh(\overline{x}_1/\epsilon)$, then then its time derivative is given by $\dot{\hat{d}} = k_1 \frac{\dot{\overline{x}}_1}{\epsilon}\left(1 - \tanh^2\left(\frac{\overline{x}_1}{\epsilon}\right)\right)$. Accordingly, an ultimate bound on $\dot{\hat{d}}$ can be found to be $\left|\dot{\hat{d}}\right| \leq \frac{k_1\left|\dot{\overline{x}}_1\right|}{\epsilon}$ at the worst case where $|\overline{x}_1| = 0$. Then,

$$\dot{V}_{\overline{x}_1} \leq -\left|\dot{\overline{x}}_1\right|\left(\frac{k_1\left|\dot{\overline{x}}_1\right|}{\epsilon} - \left|\dot{d}\right|\right) \tag{31}$$

To ensure $\dot{V}_{\overline{x}_1} \leq 0$, the following has to be satisfied:

$$\left|\dot{\overline{x}}_1\right| = \left|\dot{\overline{d}}\right| \leq \frac{\epsilon\left|\dot{d}\right|}{k_1} \tag{32}$$

Similarly, for the $\overline{\zeta}_2$

$$\left|\dot{\overline{z}}_2\right| = |\dot{\overline{\zeta}}_2| \leq \frac{\epsilon\left|\dot{\zeta}\right|}{k_2} \tag{33}$$

accordingly, the uniform ultimate boundedness can be guaranteed for $\dot{V}(z_1, z_2)$

$$\dot{V}(z_1, z_2) \leq -c\,||z||^2 + \frac{\epsilon}{k}\,||z||\,||\overline{D}_3|| \tag{34}$$

where, $||\overline{D}_3|| = k\sqrt{(\left(\frac{1}{k_1}\left|\dot{d}\right|\right)^2 + \left(\frac{1}{k_2}\left|\dot{\zeta}\right|\right)^2)}$. Letting $0 < \vartheta < 1$, one can deduce

$$\dot{V}(z_1, z_2) \leq -c\,||z||^2 + \frac{\epsilon}{k}\,||z||\,||\overline{D}_3|| + c\vartheta\,||z||^2 - c\vartheta\,||z||^2$$

$$\dot{V}(z_1, z_2) \leq -c(1-\vartheta)\,||z||^2 + \frac{\epsilon}{k}\,||z||\,||\overline{D}_3|| - c\vartheta\,||z||^2$$

$$\dot{V}(z_1, z_2) \leq -c(1-\vartheta)\,||z||^2 \;\forall\, ||z|| > \frac{\epsilon\,||\overline{D}_3||}{ck\vartheta} \tag{35}$$

Then, according to Theorem 4.18 and Lemma 9.2 in [9], the ultimate bound can finally be established

$$||z|| \leq \frac{\epsilon\,||\overline{D}_3||}{ck} \tag{36}$$

The ultimate bound of Equation (36) represents the new contribution achieved in this study, where the bound depends on the disturbance estimation error, which in turn relies on the upper bound of differentiable disturbance. The ultimate bound can be easily made arbitrarily small by selecting small approximation parameters ϵ and large k. On the basis of stability analysis, using Equations (51) and (59), the reaching phase can be avoided or crossed over by selecting ($\overline{x}_1(0) = 0$, $\overline{z}_2(0) = 0$), which means that the disturbance estimation will take place from the beginning $t \geq t_0$.

3.3. Backstepping Controller Based on QISMC (BS-QISMC)

Based on the elimination of the reaching phase, the QISMC will be fused with the backstepping controller. Considering the case of unmatched disturbance estimation and the lumped projected matched one, the estimates due to the QISMC will be used to synthesize the virtual controller of the backstepping control algorithm and this is the key improvement in the backstepping control based on quasi-integral sliding mode control (BS-QISMC).

The virtual of Equation (4) will be redesigned as

$$x_2^* = -cz_1 - ax_1 + \dot{x}_{1d} - \hat{d} \tag{37}$$

Following the previous analysis (Equations (17)–(19)), the error dynamics for e_1 becomes

$$\dot{z}_1 = -cz_1 + z_2 + d - \hat{d} \tag{38}$$

Let the sliding variable s_1 be defined as

$$s_1 = z_1 + r_1 \tag{39}$$

where $r_1(t_0) = -z_1(t_0)$, that means $s_1(t_0) = 0$. Taking the time derivative of Equation (40),

$$\dot{s}_1 = -cz_1 + z_2 + d - \hat{d} + \dot{r}_1 \tag{40}$$

let $\dot{r}_1 = cz_1 - z_2$, then Equation (41) can be rewritten as

$$\dot{s}_1 = d - \hat{d} \tag{41}$$

Regarding $\hat{d}$ to be defined as

$$\hat{d} = k_{c1} tanh(s_1/\eta_1) \tag{42}$$

where $1 \gg \eta_1 > 0 \in R$, and $k_{c1} > 0 \in R$ are design parameters. The stability analysis based on the sliding mode theory leads to:

$$s_1\dot{s}_1 \leq -|s_1|(k_{c1} tanh(s_1/\eta_1) - |d|) \leq 0, \ \ \forall\, k_{c1} > |d| \tag{43}$$

where $k_{c1} > d_1$ is a necessary condition to satisfy Equation (44). Using the same procedure followed by Equations (17) and (18), to get

$$\dot{z}_1 = -cz_1 + z_2 + \overline{d} \tag{44}$$

Regarding the second channel error $z_2 = a_2x_2 - x_2^*$, the error dynamics becomes

$$\dot{z}_2 = -a_3x_1 - a_4x_2 + \frac{1}{L_a}u - c^2z_1 + cz_2 + cd - c\hat{d} - a_1^2x_1 + a_1a_2x_2 + a_1d - \ddot{x}_{1d} + \dot{\hat{d}} \tag{45}$$

The control law can be chosen to be expressed in terms of its components as,

$$u = \frac{L_a}{a_2}(u_1 + u_2) \tag{46}$$

where u_1 is defined as

$$u_1 = a_3\, x_1 + a_4\, x_2 - \left(1 - c^2\right) z_1 - 2\, c\, z_2 + a_1^2\, x_1 - a_1a_2\, x_2 + \ddot{x}_{1d} + c\hat{d} \tag{47}$$

Equation (46) can be rewritten as

$$\dot{z}_2 = -cz_2 - z_1 + (c - a_1)d + u_2 + \dot{\hat{d}} \tag{48}$$

Let $\zeta_2 = (c - a_1)\, d + \dot{\hat{d}}$, then

$$\dot{z}_2 = -cz_2 - z_1 + u_2 + \zeta_2 \tag{49}$$

The second sliding variable is defined as

$$s_2 = z_2 + r_2 \tag{50}$$

where $r_2(t_0) = -z_2(t_0)$, and that means $s_2(t_0) = 0$. Taking the time derivative of Equation (51)

$$\dot{s}_2 = -cz_2 - z_1 + u_2 + \zeta_2 + \dot{r}_2 \tag{51}$$

let $\dot{r}_2 = cz_2 + z_1$, then Equation (52) is reduced to

$$\dot{s}_2 = u_2 + \zeta_2 \tag{52}$$

If u_2 is chosen as

$$u_2 = k_{c2} tanh(s_2/\eta_2) \tag{53}$$

where $1 \gg \eta_2 > 0 \in R$, and $k_{c2} > 0 \in R$ are design parameters. The stability analysis based on the sliding mode theory leads to:

$$s_2\dot{s}_2 \leq -|s_2|(k_{c2}\, tanh(s_2/\eta_2) - |\zeta_2|) \leq 0, \;\; \forall\, k_{c2} > |\zeta_2| \tag{54}$$

where $k_{c1} > d_2$ is a necessary condition to satisfy Equation (54). Then, Equation (49) becomes

$$\dot{z}_2 = -cz_2 - z_1 + \overline{\zeta}_2 \tag{55}$$

Recalling a similar ultimate bound determination procedure of Equation (30) to Equation (34), the unmatched disturbance estimation ultimate bound is defined as

$$\left|\overline{d}\right| \leq \frac{\eta_1 \left|\dot{d}\right|}{k_{c1}} \tag{56}$$

Similarly, for the $\overline{\zeta}_2$

$$|\overline{\zeta}_2| \leq \frac{\eta_2 \left|\dot{\zeta}\right|}{k_{c2}} \tag{57}$$

Taking the time derivative of Lyapunov candidate $V(z_1, z_2)$ of Equation (9) to have

$$\dot{V}(z_1, z_2) = -c\left(z_1^2 + z_2^2\right) + z_1\overline{d} + z_2\overline{\zeta}_2 \tag{58}$$

or

$$\dot{V}(z_1, z_2) \leq -c\,||z\,||^2 + ||z\,||\,||\overline{D}_2\,|| \tag{59}$$

where $||\overline{D}_2\,|| = \sqrt[2]{\left|\overline{d}\right|^2 + \left|\overline{\zeta}_2\right|^2}$. Letting $0 < \vartheta < 1$, then

$$\dot{V}(z_1, z_2) \leq -c(1-\vartheta)\,||z\,||^2 + ||z\,||\,||\overline{D}_2\,|| - c\vartheta\,||z\,||^2$$

or

$$\dot{V}(z_1, z_2) \leq -c(1-\vartheta)\,||z\,||^2 \;\; \forall ||z\,|| > \frac{||\overline{D}_2\,||}{c\vartheta} \tag{60}$$

Referring to Ref. [2] (Theorem 4.18 and Lemma 9.2), the ultimate bound is

$$||z\,|| \leq \rho\left(\frac{||\overline{D}_2\,||}{c}\right) \leq \frac{||\overline{D}_2\,||}{c} \tag{61}$$

The ultimate bound of Equation (61) represents a considerable achievement where the bound depends on the disturbance estimation error.

4. Discussion and Simulation Results

The proposed controllers' verification for the DC motor-driven EV system has been made based on numerical simulation using MATLAB (2020). The setting of DC motor parameters used in the simulation results are considered from a scaled-down real platform listed in Table 1.

Table 1. DC motor system parameters.

Parameters	Values	Units
J	7.95×10^{-5}	kg·m^2/rad
L_a	105×10^{-6}	H
R_a	0.7	Ω
b	0	N·m·s/rad
K_b	59×10^{-3}	N·m/A or V·s/rad

The desired speed trajectory can be described as follows

$$x_{1d} = \begin{cases} 104.72 & 0 \leq t \leq 3 \\ 136.13 & 3 \leq t \leq 7 \\ 115.2 & 7 \leq t \end{cases} \quad \text{rad/s}$$

The load torque is considered as a shifted sinusoidal signal as: $T_l = 0.05 + 0.03\ \sin(0.6\pi t) + 0.02\ \sin(2\pi t)$ (Nm). For all controllers, the design parameters are chosen as $c = 200$, $k_{c1} = k_1 = 1300$, $k_{c2} = k_2 = 755,000$, $\epsilon_1 = \eta_1 = 0.05$, and $\epsilon_2 = \eta_2 = 5$. The initial conditions of $x_1(0) = 0$ and $x_2(0) = 0$. The control objective is to ensure the smallest ultimate bound of error convergence of the state ω to the ω_d (or to the smallest ultimate bound).

Figure 3 shows the time response of rotor angular speed ω represented by the state x_1 for the two controllers BS-QSMDO and BS-QISMC. In terms of transient characteristics, the BS-QSMDO shows the highest peak overshoot as compared to other controllers. On the other hand, BS-QISMC has no overshoot. However, the response of BS-QSMDO is faster than that based on BS-QISMC. Figure 4 shows the behavior of tracking error e_1 based on the two controllers and it is clear that the two controllers give approximately the same steady-state error. Table 2 reports the RMS of the tracking error.

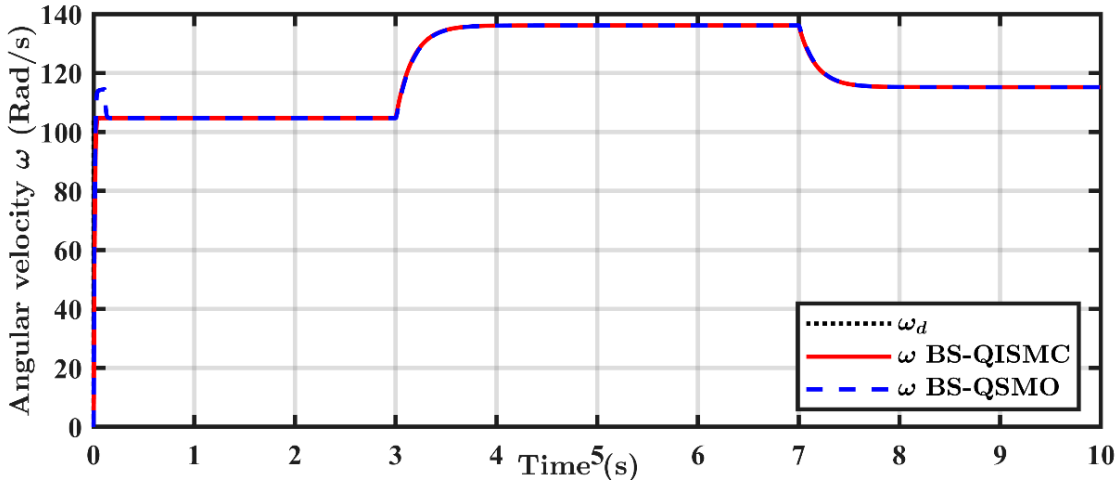

Figure 3. The behavior of x_1 for the suggested controllers.

Table 2. Performance characteristics.

Controller	RMS of Variables			
	z_1	z_2	u	$T_l - \hat{T}_l$
BS-QISMC	2.6401	327.3881	6.5568	7.1404×10^{-5}
BS-QSMO	2.6307	349.9241	6.5624	5.4685×10^{-6}

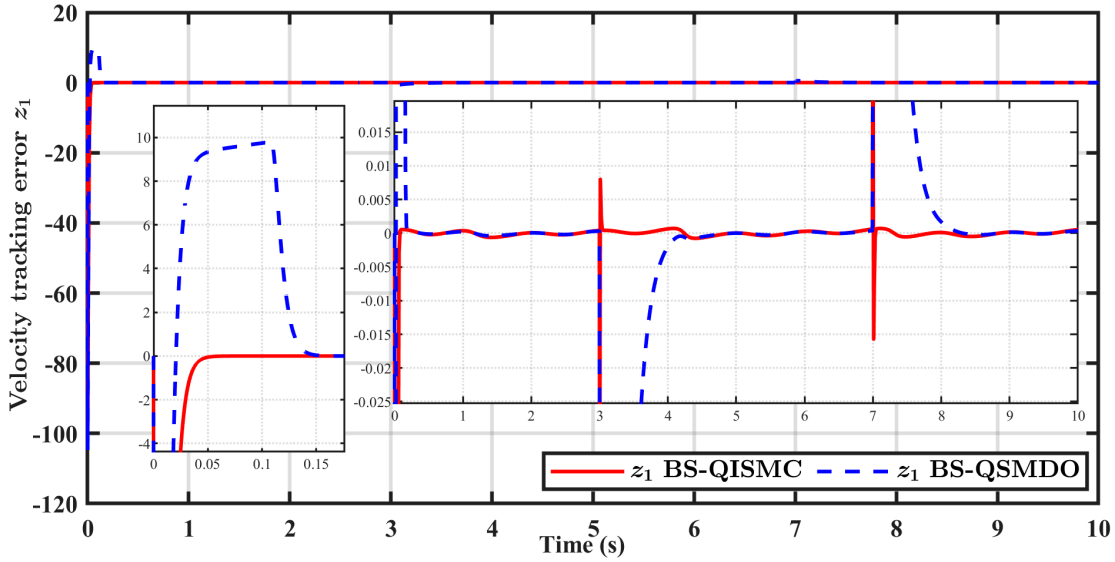

Figure 4. The behavior of z_1 for the suggested controllers.

Figure 5 shows the behaviors of control actions due to the proposed controllers. It is evident that the controlled system based on BS-QSMDO has the highest initial control effort as compared to the other controller. The evaluation of control efforts based on the proposed controllers in RMS is also reported in Table 2. Figure 6 shows the tracking error z_2 of the lower subsystem. The transient error of BS-QSMDO is higher than that of BS-QISMC, as shown in the RMS value in Table 2; however, to the naked eye, the error is approximately the same for both the controllers in the steady state.

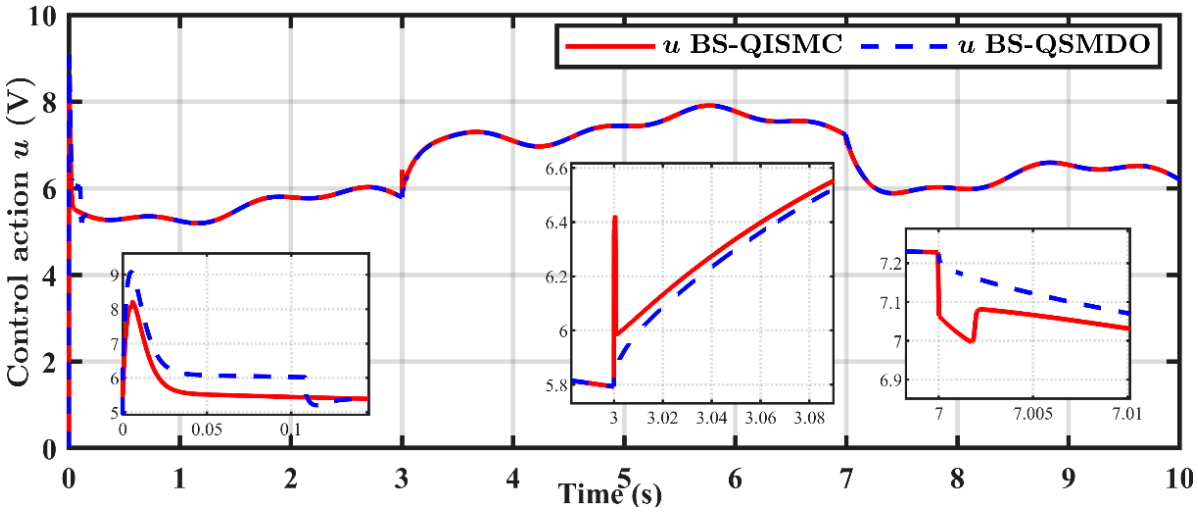

Figure 5. Control action u for the proposed observer-based controllers.

Figure 7 shows the responses of armature currents i_a, represented by state variable x_2, due to the proposed controllers. It is worth mentioning that the state x_2 tries to strictly follow the virtual controller, which in turn enables the state variable x_1 to track the desired speed. According to the figure, one can observe that the highest initial current can be produced by the BS-QSMDO controller, while the other controller gives lower initial values for armature current.

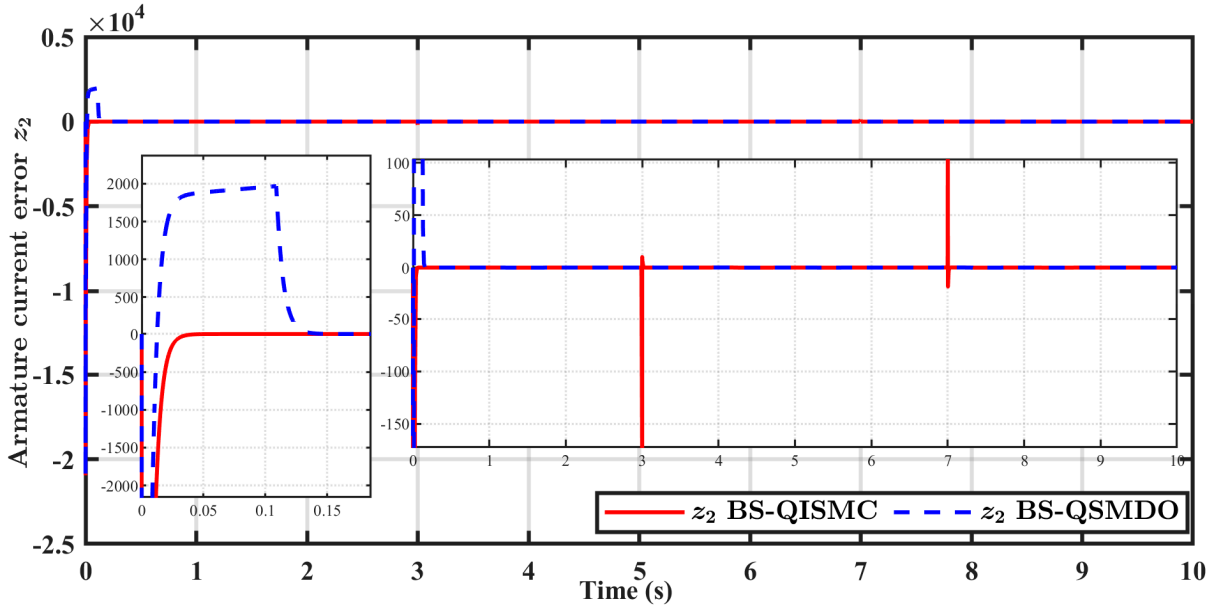

Figure 6. Armature current error z_2 for the suggested controllers.

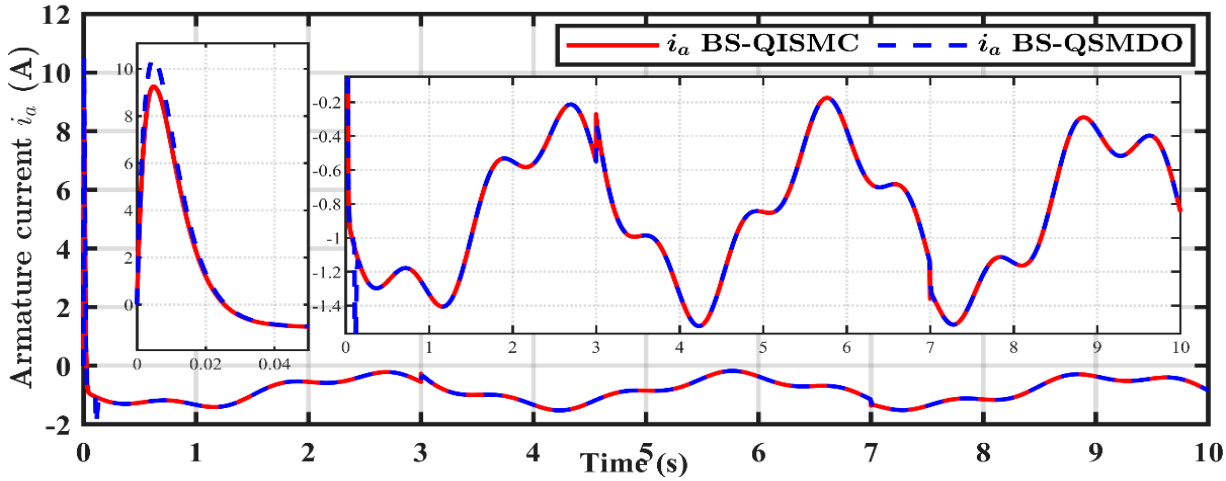

Figure 7. The behavior of x_2 for the proposed controllers.

Figures 8 and 9 show the state and error estimation errors based on QSMDO. The ultimate boundedness of the estimation error is obvious from the figures with a focus on the state x_1 due to considering the control problem relative to output tracking control. Figure 10 shows the actual load torque and its estimates resulting from QSMDO and QISMC. One can see that they are capable of estimating the load torque with considerably small errors. However, QSMDO shows the lowest disturbance estimation error. Figure 11 shows the estimation error between the actual load torque T_l and its estimate $\hat{T}_l$. As previously proved in the stability analysis, it is clear that the ultimate bound can be reached by both of the proposed controllers. However, the ultimate bound produced by BS-QSMO is lower as compared to that of BS-QISMC, as shown by the RMS value of the estimation error in Table 2.

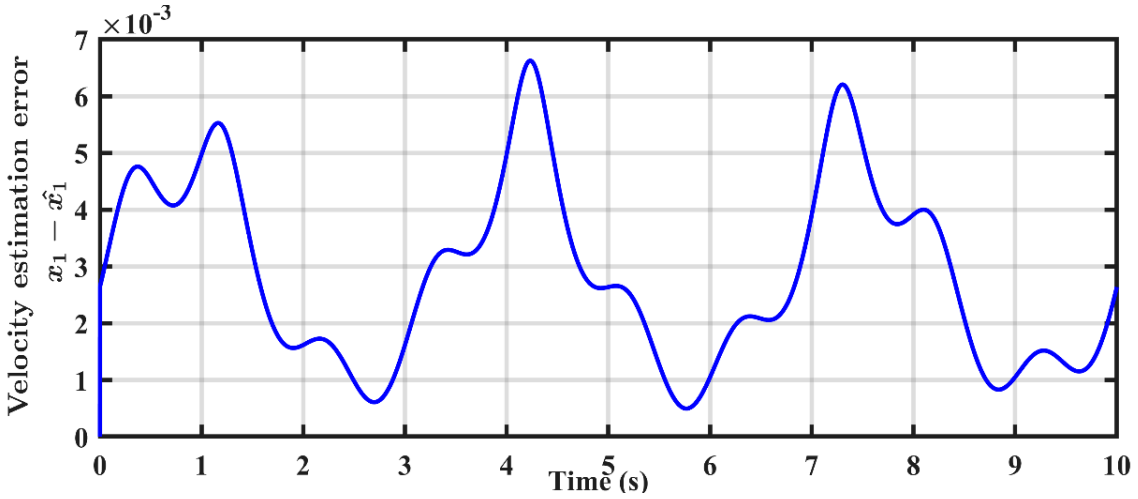

Figure 8. State estimation x_1, $\hat{x}_1$ for BS-QSMDO controller.

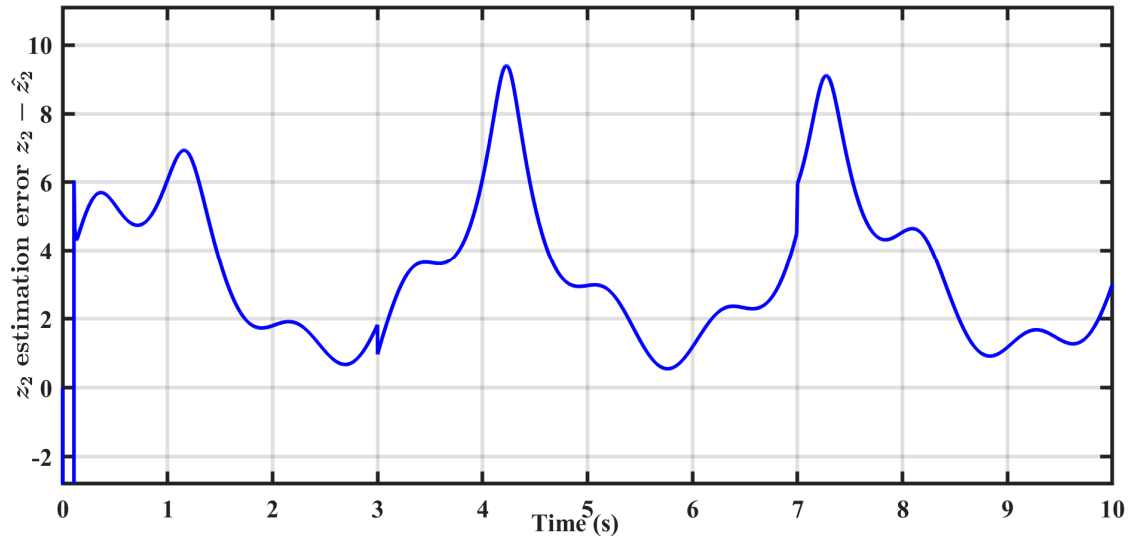

Figure 9. State estimation z_2, $\hat{z}_2$ for BS-QSMDO controller.

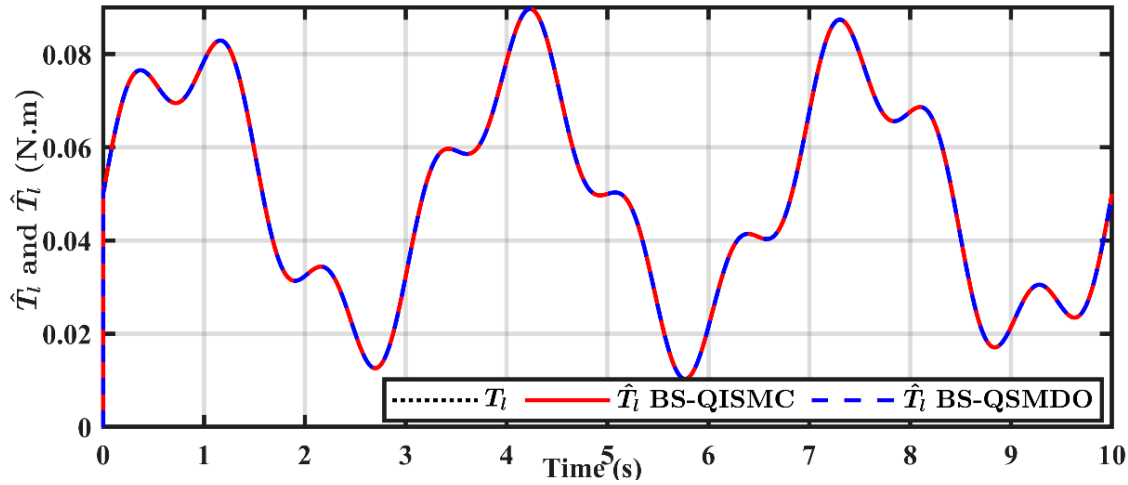

Figure 10. The behaviors of actual torque T_l and estimated torque $\hat{T}_l$.

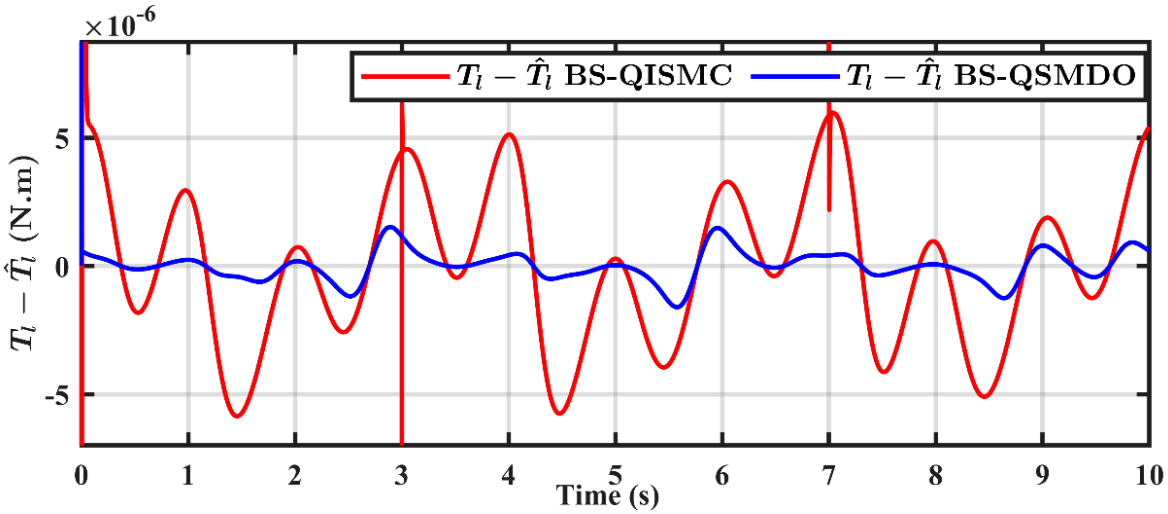

Figure 11. The estimation errors ($T_l - \hat{T}_l$).

5. Conclusions

This paper has addressed the control problem of an EV driven by a DC motor under unmatched disturbance (road friction torque). This study has adopted two control schemes to solve this problem: backstepping control based on quasi-sliding mode disturbance observer (BS-QSMO) and backstepping control based on quasi-integral sliding mode control (BS-QISMC). A rigorous stability analysis has been developed to determine the ultimate boundedness of tracking and estimation errors for both control approaches. A comparison study has been made between BS-QSMO and BS-QISMC in terms of tracking and estimation error convergences. The numerical simulation was conducted to verify the effectiveness of the proposed controllers in the sense of error convergence. The RMS criterion has been used as a performance-evaluating index for the proposed control schemes in terms of estimation errors, tracking errors, and control efforts. Compared to BS-QISMC, the results showed that a lower (by 0.36%) level of ultimate boundedness with a higher convergent rate can be reached using BS-QSMO. However, a higher level of control effort of 0.0853% can be observed with BS-QSMO as compared to the other controller, and this is the price to be paid by the BS-QSMO controller to achieve a lower ultimate boundedness with a faster convergence rate. In order to extend this study for future work, the numerical results can be validated in a real-world environment. The embedded system design either based on a field programming gate array (FPGA), Raspberry Pi board, or LabVIEW-based hardware is the potential solution for real-world implementation. Moreover, intermediate concerns and challenges can be addressed like the robustness analysis in the presence of time delays and saturation of control effort. It is also interesting to conduct a control design study for a dynamic model for a four-wheel drive vehicle instead of a one-motor actuated car. This will significantly increase reliability and survivability, controllability and safety, reduce tire wear, and increase efficiency.

Author Contributions: Conceptualization, S.A.A.-S.; formal analysis, A.H.H.; funding acquisition, N.S.; methodology, A.H.H. and S.A.A.-S.; software, A.H.H.; supervision, S.A.A.-S. and A.J.H.; writing—original draft, A.H.H.; writing—review and editing, A.J.H. All authors have read and agreed to the published version of the manuscript.

Funding: This research received no external funding.

Data Availability Statement: The original contributions presented in the study are included in the article, further inquiries can be directed to the corresponding author.

Conflicts of Interest: Akram Hashim Hameed is employee of Al-Sader Branch, Baghdad State Company of Electricity Distribution, Ministry of Electricity. The paper reflects the views of the scientists and not the company.

References

1. Kaarlela, T.; Villagrossi, E.; Rastegarpanah, A.; San-Miguel-Tello, A.; Pitkäaho, T. Robotised disassembly of electric vehicle batteries: A systematic literature review. *J. Manuf. Syst.* **2024**, *74*, 901–921. [CrossRef]
2. Shchurov, N.I.; Dedov, S.I.; Malozyomov, B.V.; Shtang, A.A.; Martyushev, N.V.; Klyuev, R.V.; Andriashin, S.N. Degradation of lithium-ion batteries in an electric transport complex. *Energies* **2021**, *14*, 8072. [CrossRef]
3. Girardi, P.; Brambilla, P.C. *Electric Cars vs. Diesel and Gasoline: A Comparative LCA Ranging from MicroCar to Family Car*; Academic Star Publishing Company: New York, NY, USA, 2019.
4. Kosuru, V.S.R.; Kavasseri Venkitaraman, A. Trends and challenges in electric vehicle motor drivelines-A review. *Int. J. Electr. Comput. Eng. Syst.* **2023**, *14*, 485–495.
5. Akhtar, N.; Patil, V. Electric vehicle technology: Trends and challenges. In *Proceedings of the International Conference on Smart Technologies for Energy, Environment, and Sustainable Development*; Springer: Berlin/Heidelberg, Germany, 2020; pp. 621–637.
6. Ahmed, A.K.; Al-Khazraji, H. Optimal control design for propeller pendulum systems using gorilla troops optimization. *J. Eur. Syst. Autom.* **2023**, *56*, 575–582. [CrossRef]
7. Jin, X.; Wang, Q.; Yan, Z.; Yang, H. Nonlinear robust control of trajectory-following for autonomous ground electric vehicles with active front steering system. *AIMS Math* **2023**, *8*, 11151–11179. [CrossRef]
8. Zouari, F.; Ibeas, A.; Boulkroune, A.; Cao, J. Finite-time adaptive event-triggered output feedback intelligent control for noninteger order nonstrict feedback systems with asymmetric time-varying Pseudo-state constraints and nonsmooth input nonlinearities. *Commun. Nonlinear Sci. Numer. Simul.* **2024**, *136*, 108036. [CrossRef]
9. Humaidi, A.J.; Hasan, S.; Al-Jodah, A.A. Design of second order sliding mode for glucose regulation systems with disturbance. *Int. J. Eng. Technol. (UAE)* **2018**, *7*, 243–247. [CrossRef]
10. Hussein, E.Q.; Al-Dujaili, A.Q.; Ajel, A.R. Design of sliding mode control for overhead crane systems. *Proc. IOP Conf. Ser. Mater. Sci. Eng.* **2020**, *881*, 012084. [CrossRef]
11. Al-Ani, A.; Seitz, J. An approach for QoS-aware routing in mobile ad hoc networks. In Proceedings of the 2015 International Symposium on Wireless Communication Systems (ISWCS), Brussels, Belgium, 25–28 August 2015; pp. 626–630.
12. Rakan, A.B.; Ridha, T.M.; Al-Saamray, S.A. Automatic glycemia regulation: Avoiding hypoglycemia and hyperglycemia. In Proceedings of the International Conference on Communication and Information Technology, ICICT 2021, Basrah, Iraq, 5–6 June 2021; Institute of Electrical and Electronics Engineers Inc.: Piscataway, NJ, USA, 2021; pp. 74–79.
13. Salman, A.D.; Khudheer, U.; Abdulsaheb, G.M. An adaptive smart street light system for smart city. *J. Comput. Theor. Nanosci.* **2019**, *16*, 262–268. [CrossRef]
14. M Raafat, S.; Akmeliawati, R. Survey on robust control of precision positioning systems. *Recent Pat. Mech. Eng.* **2012**, *5*, 55–68. [CrossRef]
15. Raafat, S.M.; Martono, W.; Akmeliawati, R. comparative study of parametric and intelligent unstructured uncertainties for robust controller design. In Proceedings of the 2009 IEEE Symposium on Industrial Electronics & Applications, Kuala Lumpur, Malaysia, 4–6 October 2009; IEEE: Piscataway, NJ, USA, 2009; pp. 259–264.
16. Humaidi, A.J.; Hameed, A.H. Robustness Enhancement of MRAC Using Modification Techniques for Speed Control of Three Phase Induction Motor. *J. Electr. Syst.* **2017**, *13*, 723–741.
17. Zouari, F.; Boubellouta, A. Adaptive neural control for unknown nonlinear time-delay fractional-order systems with input saturation. In *Advanced Synchronization Control and Bifurcation of Chaotic Fractional-Order Systems*; IGI Global: Hershey, PA, USA, 2018; pp. 54–98.
18. Estrada, A.; Fridman, L.M. Integral HOSM Semiglobal Controller for Finite-time Exact Compensation of Unmatched Perturbations. *IEEE Trans. Autom. Control* **2010**, *55*, 2645–2649. [CrossRef]
19. Mattei, G.; Monaco, S. Robust backstepping control of missile lateral and rolling motions in the presence of unmatched uncertainties. In Proceedings of the 2012 IEEE 51st IEEE Conference on Decision and Control (CDC), Maui, HI, USA, 10–13 October 2012; IEEE: Piscataway, NJ, USA, 2009; pp. 2878–2883.
20. Hassan, M.Y.; Humaidi, A.J.; Hamza, M.K. On the design of backstepping controller for Acrobot system based on adaptive observer. *Int. Rev. Electr. Eng.* **2020**, *15*, 328–335. [CrossRef]
21. Bacha, S.; Saadi, R.; Ayad, M.Y.; Sahraoui, M.; Laadjal, K.; Cardoso, A.J.M. Autonomous electric-vehicle control using speed planning algorithm and back-stepping approach. *Energies* **2023**, *16*, 2459. [CrossRef]
22. Castanos, F.; Fridman, L. Analysis and Design of Integral Sliding Manifolds for Systems with Unmatched Perturbations. *IEEE Trans. Autom. Control* **2006**, *51*, 853–858. [CrossRef]
23. Zouari, F.; Saad, K.B.; Benrejeb, M. Adaptive backstepping control for a single-link flexible robot manipulator driven DC motor. In Proceedings of the 2013 International Conference on Control, Decision and Information Technologies (CoDIT), Hammamet, Tunisia, 6–8 May 2013; IEEE: Piscataway, NJ, USA, 2013; pp. 864–871.
24. Merazka, L.; Zouari, F.; Boulkroune, A. High-gain observer-based adaptive fuzzy control for a class of multivariable nonlinear systems. In Proceedings of the 2017 6th International Conference on Systems and Control (ICSC), Batna, Algeria, 7–9 May 2017; IEEE: Piscataway, NJ, USA, 2017; pp. 96–102.
25. Saleh, A.K.; Al-Zughaibi, A.I.; Hussein, E.Q. Develop a servo actuator system adaptive sliding mode controller. *AIP Conf. Proc.* **2023**, *2977*, 030023.

26. Rigatos, G.; Abbaszadeh, M.; Sari, B.; Siano, P.; Cuccurullo, G.; Zouari, F. Nonlinear optimal control for a gas compressor driven by an induction motor. *Results Control Optim.* **2023**, *11*, 100226. [CrossRef]
27. Al-Khazraji, H.; Naji, R.M.; Khashan, M.K. Optimization of Sliding Mode and Back-Stepping Controllers for AMB Systems Using Gorilla Troops Algorithm. *J. Eur. Systèmes Autom.* **2024**, *57*, 417–424. [CrossRef]
28. Ahmed, M.; Masood, U.; Azeem, M.K.; Ahmad, I.; Jabbar, A.U. Barrier function based adaptive sliding mode controller for the hybrid energy storage system of plugin hybrid electric vehicles. *J. Energy Storage* **2023**, *72*, 108051. [CrossRef]
29. Aljuboury, A.S.; Hameed, A.H.; Ajel, A.R.; Humaidi, A.J.; Alkhayyat, A.; Mhdawi, A.K.A. Robust Adaptive Control of Knee Exoskeleton-Assistant System Based on Nonlinear Disturbance Observer. *Actuators* **2022**, *11*, 78. [CrossRef]
30. Al-Samarrai, S.A.; Al-Nadawi, Y.K.; Hama, T.G.; Al-Gadery, T.A. Robust Adaptive Sliding Mode Controllers Design for a Non-holonomic Mobile Robot. *Stud. Comput. Intell.* **2023**, *1090*, 489–556. [CrossRef]
31. Ao, D.; Wong, P.K.; Huang, W. Model predictive control allocation based on adaptive sliding mode control strategy for enhancing the lateral stability of four-wheel-drive electric vehicles. *Proc. Inst. Mech. Eng. Part D J. Automob. Eng.* **2024**, *238*, 1514–1534. [CrossRef]
32. Rahman, M.H.; Al-Zughaibi, A.I.; Hussein, E.Q. Design of robust control strategy for nonlinear wind turbine under parametric uncertainty. *AIP Conf. Proc.* **2023**, *2804*, 030003.
33. Kang, S.; Chen, J.; Qiu, G.; Tong, H. Slip Ratio Adaptive Control Based on Wheel Angular Velocity for Distributed Drive Electric Vehicles. *World Electr. Veh. J.* **2023**, *14*, 119. [CrossRef]
34. Al-Khazraji, H. Comparative study of whale optimization algorithm and flower pollination algorithm to solve workers assignment problem. *Int. J. Prod. Manag. Eng.* **2022**, *10*, 91–98. [CrossRef]
35. Al-Zughaibi, A.I.; Hussein, E.Q.; Huseein, N.A. Simulation study of a linear quadratic control for active seat suspension systems. *AIP Conf. Proc.* **2023**, *2631*, 030005.
36. Shtessel, Y.; Edwards, C.; Fridman, L.; Levant, A. *Sliding Mode Control and Observation*; Springer: Berlin/Heidelberg, Germany, 2014; Volume 10.
37. Zouari, F.; Boulkroune, A.; Ibeas, A.; Arefi, M.M. Observer-based adaptive neural network control for a class of MIMO uncertain nonlinear time-delay non-integer-order systems with asymmetric actuator saturation. *Neural Comput. Appl.* **2017**, *28*, 993–1010. [CrossRef]
38. Hamad, Q.M.; Raafat, S.M. A flatness-based trajectory tracking control for chemical reactor. In Proceedings of the 2024 21st International Multi-Conference on Systems, Signals & Devices (SSD), Erbil, Iraq, 22–25 April 2024; IEEE: Piscataway, NJ, USA, 2024; pp. 819–825.
39. Haddad, M.; Zouari, F.; Boulkroune, A.; Hamel, S. Variable-structure backstepping controller for multivariable nonlinear systems with actuator nonlinearities based on adaptive fuzzy system. *Soft Comput.* **2019**, *23*, 12277–12293. [CrossRef]
40. Saleh, A.K.; Al-Zughaibi, A.I.; Hussein, E.Q. Using an adaptive sliding mode control to improve control in hydraulic servo systems. *AIP Conf. Proc.* **2024**, *3091*, 050006.
41. Zouari, F.; Ibeas, A.; Boulkroune, A.; Cao, J.; Arefi, M.M. Adaptive neural output-feedback control for nonstrict-feedback time-delay fractional-order systems with output constraints and actuator nonlinearities. *Neural Netw.* **2018**, *105*, 256–276. [CrossRef]
42. Utkin, V.; Guldner, J.; Shi, J. *Sliding Mode Control in Electro-Mechanical Systems*; CRC Press: Boca Raton, FL, USA, 2017.
43. Humaidi, A.J.; Talaat, E.N.; Hameed, M.R.; Hameed, A.H. Design of Adaptive Observer-Based Backstepping Control of Cart-Pole Pendulum System. In Proceedings of the 2019 3rd IEEE International Conference on Electrical, Computer and Communication Technologies, ICECCT 2019, Tamil Nadu, India, 20–22 February 2019; Institute of Electrical and Electronics Engineers Inc.: Piscataway, NJ, USA, 2019. [CrossRef]
44. Al-Samarraie, S.A.; Midhat, B.F.; Gorial, I.I. Nonlinear integral control design for DC motor speed control with unknown and variable external torque. *J. Eng. Sustain. Dev.* **2016**, *20*, 19–33.
45. Mahmood, Z.N.; Al-Khazraji, H.; Mahdi, S.M. Adaptive control and enhanced algorithm for efficient drilling in composite materials. *J. Eur. Systèmes Autom.* **2023**, *56*, 507–512. [CrossRef]
46. Boumegouas MK, B.; Kouzi, K.; Birame, M.H. Robust synergetic control of electric vehicle equipped with an improved load torque observer. *Int. J. Emerg. Electr. Power Syst.* **2024**, *25*, 197–205. [CrossRef]
47. Ekinci, S.; Izci, D.; Hekimoğlu, B. PID speed control of DC motor using Harris hawks optimization algorithm. In Proceedings of the 2020 International Conference on Electrical, Communication, and Computer Engineering (ICECCE), Istanbul, Turkey, 12–13 June 2020; IEEE: Piscataway, NJ, USA, 2020; pp. 1–6.
48. Talib, A.A.; Salman, A.D. Design and develop authentication in electronic payment systems based on IoT and biometric. *Telkomnika (Telecommun. Comput. Electron. Control.)* **2022**, *20*, 1297–1306. [CrossRef]
49. Hoyos, F.E.; Candelo-Becerra, J.E.; Hoyos Velasco, C.I. Application of zero average dynamics and fixed point induction control techniques to control the speed of a DC motor with a Buck converter. *J. Appl. Sci.* **2020**, *10*, 1807. [CrossRef]
50. Lotfy, A.; Kaveh, M.; Mosavi, M.; Rahmati, A. An enhanced fuzzy controller based on improved genetic algorithm for speed control of DC motors. *J Analog Integr. Circuits Signal Process.* **2020**, *105*, 141–155. [CrossRef]
51. Maghfiroh, H.; Sujono, A.; Apribowo, C.H.B. Basic tutorial on sliding mode control in speed control of DC-motor. *J. Electr. Electron. Inf. Commun. Technol.* **2020**, *2*, 1–4. [CrossRef]

52. Rauf, A.; Zafran, M.; Khan, A.; Tariq, A.R. Finite-time nonsingular terminal sliding mode control of converter-driven DC motor system subject to unmatched disturbances. *J. Int. Trans. Electr. Energy Syst.* **2021**, *31*, e13070. [CrossRef]
53. Humaidi, A.J.; Kadhim, S.K.; Gataa, A.S. Development of a Novel Optimal Backstepping Control Algorithm of Magnetic Impeller-Bearing System for Artificial Heart Ventricle Pump. *Cybern. Syst.* **2020**, *51*, 521–541. [CrossRef]
54. Abdul-Adheem, W.R.; Azar, A.T.; Ibraheem, I.K.; Humaidi, A.J. Novel active disturbance rejection control based on nested linear extended state observers. *Appl. Sci.* **2020**, *10*, 4069. [CrossRef]
55. Roldán-Caballero, A.; Hernández-Marquez, E.; Marciano-Melchor, M.; García-Sánchez, J.R.; Silva-Ortigoza, G. Hierarchical Flatness-Based Control for Velocity Trajectory Tracking of the "DC/DC Boost Converter–DC Motor" System Powered by Renewable Energy. *IEEE Access* **2023**, *11*, 32464–32475.
56. Patil, M.D.; Vadirajacharya, K.; Khubalkar, S.W. Design and tuning of digital fractional-order PID controller for permanent magnet DC motor. *IETE J. Res.* **2023**, *69*, 4349–4359. [CrossRef]
57. Humaidi, A.J.; Hameed, M.R. Design and performance investigation of block-backstepping algorithms for ball and arc system. In Proceedings of the 2017 IEEE International Conference on Power, Control, Signals and Instrumentation Engineering (ICPCSI), Chennai, India, 21–22 September 2017; IEEE: Piscataway, NJ, USA, 2017; pp. 325–332. [CrossRef]
58. Zouari, F.; Saad, K.B.; Benrejeb, M. Robust adaptive control for a class of nonlinear systems using the backstepping method. *Int. J. Adv. Robot. Syst.* **2013**, *10*, 166. [CrossRef]
59. Zouari, F.; Saad, K.B.; Benrejeb, M. Adaptive internal model control of a DC motor drive system using dynamic neural network. *J. Softw. Eng. Appl.* **2012**, *5*, 18298. [CrossRef]